Polarization locked vector solitons and axis instability in optical fiber

Steven T. Cundiff[a)]
JILA, University of Colorado and National Institute of Standards and Technology, Boulder, Colorado 80309-0440

Brandon C. Collings
Bell Laboratories, Lucent Technologies, Holmdel, New Jersey 07733

Keren Bergman
Department of Electrical Engineering, Princeton University, Princeton, New Jersey 08544

(Received 24 November 1999; accepted for publication 31 March 2000)

We experimentally observe polarization-locked vector solitons in optical fiber. Polarization locked-vector solitons use nonlinearity to preserve their polarization state despite the presence of birefringence. To achieve conditions where the delicate balance between nonlinearity and birefringence can survive, we studied the polarization evolution of the pulses circulating in a laser constructed entirely of optical fiber. We observe two distinct states with fixed polarization. This first state occurs for very small values birefringence and is elliptically polarized. We measure the relative phase between orthogonal components along the two principal axes to be $\pm\pi/2$. The relative amplitude varies linearly with the magnitude of the birefringence. This state is a polarization locked vector soliton. The second, linearly polarized, state occurs for larger values of birefringence. The second state is due to the fast axis instability. We provide complete characterization of these states, and present a physical explanation of both of these states and the stability of the polarization locked vector solitons. © *2000 American Institute of Physics.* [S1054-1500(00)00103-8]

Although optical fiber is not truly isotropic, i.e., it always displays small amounts of random birefringence, the propagation of optical solitons is usually discussed without including polarization. While solitons are robust against the differing group velocity caused by weak birefringence, in general their polarization evolves as they propagate. By studying the polarization evolution of a soliton circulating inside a fiber laser, we observe that, for the certain nonzero values of round-trip birefringence, the polarization is fixed. Locking of the polarization occurs for very low values of birefringence, in which case the output is elliptically polarized. This corresponds to the formation of a polarization locked vector soliton (PLVS). Based on the stability mechanism, a PLVS is expected to be elliptically polarized, with a $\pm\pi/2$ phase difference between orthogonal components and an amplitude ratio that varies linearly with birefringence. We experimentally verify these properties. Locking of the polarization also occurs for larger values of birefringence, but here the output is linearly polarized. We show that the polarization direction is aligned along the slow axis of the cavity. Based on this, we attribute this behavior to axis instability, which only requires high intensity and is not incumbent on the presence of solitons.

I. INTRODUCTION

The existence of solitons in optical fiber was first predicted by Hasegawa and Tappert in 1973.[1] Solitons propagate without distortion of either their pulse shape or spectrum by balancing anomalous group velocity dispersion against self-phase modulation due to the (Kerr) nonlinear index of refraction. Their propagation is described by the (scalar) nonlinear-Schrödinger equation (NLSE). This pioneering paper ignored the fact that all ''single'' mode optical fiber actually supports two orthogonal polarization modes; the term ''single'' mode refers only to the transverse profile. If optical fiber where perfectly isotropic, the polarization modes would be completely degenerate and this treatment would be justified. In reality, manufacturing imperfections, externally applied stress, or bending lifts the degeneracy between the modes. Thus fiber supports two orthogonally polarized modes with differing propagation constants, i.e., fiber is birefringent.[2] The experimental observation of optical solitons[3] and the subsequent explosion of work[4] proved that this omission was nevertheless justified.

The difference between the phase velocities of the two modes causes the polarization state of a pulse to evolve as it propagates. Furthermore, the group velocities are also, in general, unequal. The differing group velocities result in temporal pulse splitting, a phenomena known as polarization mode dispersion and currently of great concern for nonsoliton long distance optical communication systems.[5] The differing group velocities might also be expected to prevent the formation of a soliton with energy in both orthogonal polarization modes (i.e., along both principal axes of the birefringence). However solitons are remarkably robust; they do exist under these conditions and propagate as a unit.[6] To cancel the group velocity difference, the orthogonally polarized components of the soliton shift their center frequency slightly. This phenomenon has been described theoretically using a pair of coupled nonlinear Schrödinger equations.[7–9]

[a)]Staff member, Quantum Physics Division, National Institute of Standards and Technology.

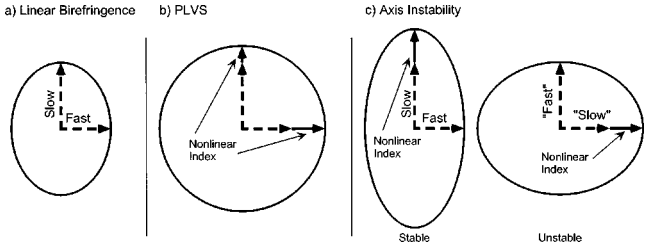

FIG. 1. Schematic of the interplay between linear and nonlinear birefringence. (a) Linear birefringence alone; (b) balance between linear and nonlinear birefringence that occurs for a PLVS; (c) conditions for the fast axis to become unstable. The ellipses are an aid for visualizing the relative magnitude of the indices of refraction.

Since the phase velocities are still different, the polarization state evolves with propagation.

The term ''vector soliton'' refers to a multidimensional entity that propagates in an invariant or periodic manner in an environment that is destructive in the absence of compensating nonlinearity.[10] The situation described above can be denoted as a group-velocity locked vector soliton as it contains amplitude along both principal axes and is therefore multidimensional.

In this paper, we review our work on the experimental observation of vector solitons that display locking of the phase velocities in addition to the group velocities. Prior to our observation, such states had only been characterized theoretically.[11–16] These states are elliptically polarized and they exist due to a dynamic balance between linear and nonlinear birefringence. The nonlinear birefringence arises from a combination of self- and cross-phase-modulation. This balance is shown schematically in Fig. 1(b). Coherent energy coupling (also called four-wave-mixing) provides a stabilizing mechanism that maintains the exact power distribution for the balance to occur. We call these states polarization-locked vector solitons (PLVS) as they have power along both principal axes, thereby being multidimensional.

In addition to the PLVS, we also observe states with fixed linear polarization. These occur at larger values of birefringence than the PLVS. These are due to axis instabilities.[17–19] Axis instabilities arise when the nonlinear birefringence can cause the phase velocity of the fast axis to become comparable or slower than that of the slow axis [see Fig. 1(c)]. In this case, the fast axis becomes unstable.

We first observed that the polarization state in a fiber laser could spontaneously lock, although the mechanisms were unclear.[20] This triggered theoretical work to show that the PLVS, predicted for strictly conservative systems,[11–16] could exist in the nonconservative environment of a fiber laser.[21] Based on this theoretical work, we were able to positively identify the polarization locked states that were occurring.[22–24]

II. THEORETICAL BACKGROUND

The full vector model describing the propagation of the two components polarized along the orthogonal principal axes of a lossless fiber are given by the conservative coupled nonlinear Schrödinger equations (CNLSE),[7,25]

$$i\frac{\partial u}{\partial z}+i\delta\frac{\partial u}{\partial t}+\gamma u+\frac{1}{2}\frac{\partial^2 u}{\partial t^2}+(|u|^2+A|v|^2)u+Bv^2u^*=0, \tag{1a}$$

$$i\frac{\partial v}{\partial z}-i\delta\frac{\partial v}{\partial t}-\gamma v+\frac{1}{2}\frac{\partial^2 v}{\partial t^2}+(|v|^2+A|u|^2)v+Bu^2v^*=0, \tag{1b}$$

where u and v are the component envelopes along the slow and fast axes, respectively, z and t are the normalized time and distance, 2δ and 2γ are the normalized group and phase velocity differences, and A and B are the cross phase modulation and coherent energy exchange coefficients, respectively.

These equations admit two linearly polarized fundamental soliton solutions,

$$u(t,z)=u_0\ \mathrm{sech}(t-\delta z)\exp(i\gamma z)\quad v(t,z)=0, \tag{2a}$$

$$u(t,z)=0\quad v(t,z)=v_0\,\mathrm{sech}(t+\delta z)\exp(i\gamma z). \tag{2b}$$

For an isotropic and conservative medium, $B=1-A$ in Eqs. (1a) and (1b). When $A=1$ [the self phase modulation (SPM) and cross phase modulation (XPM) coefficients are equal and the coherent energy exchange vanishes] and $\delta=0$, the CNLSE are integrable with stationary phase locked solutions.[26] The experimental observation of these simple hyperbolic secant shaped solutions, known as ''Manakov'' solitons, is difficult as $A\neq 1$ for most low-loss materials. Through engineering of the SPM and XPM coefficients in an anisotropic waveguide ($A\sim 0.95$), spatial ''Manakov'' solitons have been observed.[27] Spatial solitons are governed by CNLSE analogous to Eqs. (1a) and (1b). In isotropic media such as standard single mode fiber, $A=2/3$ and rigorous temporal ''Manakov'' solitons cannot occur.

In the case where the linear birefringence is significantly larger than the nonlinear birefringence, the relative optical phase between components varies so rapidly that all phase dependent phenomena effectively average to zero with propagation.[7] Thus, the coherent energy coupling and phase velocity difference terms in Eqs. (1a) and (1b) can be ignored, resulting in the only coupling between the two components being due to incoherent XPM. In this case, the solutions approximate ''Manakov'' solitons. We will call this condition ''high birefringence.'' It occurs in single mode fiber (SMF) if the peak power is less than 1 W or in polarization maintaining fiber, which has very large birefringence intentionally manufactured into it. For high birefringence, the solutions to Eqs. (1a) and (1b) correspond to two orthogonally polarized pulses along the birefringent axes that mutually trap each other. They propagate as a nondispersing group velocity locked vector soliton.[8,10] The XPM causes the central optical frequency of one component to increase and the other to decrease. In conjunction with a frequency dependent group velocity, these shifts equalize their group velocities.[7] In the absence of nonlinearity (i.e., XPM), the components will retain their central frequencies and travel at unequal group velocities, which cause them to split temporally. Due to the large phase velocity difference between the components, the polarization state of this vector soliton evolves rapidly with propagation. At any given point, the

same polarization state applies to the entire pulse because the two components have the same amplitude and phase profiles.[28] Standards soliton communications systems operate in this high birefringent regime and utilize these group velocity locked vector solitons. Hence, these soliton systems are relatively immune to the detrimental pulse splitting effects of random and unequal group velocities (polarization mode dispersion) that often impairs the performance on nonsoliton communications systems.[5,29]

We will use the designation ''low birefringence'' when the linear and nonlinear birefringence are comparable (the latter depends on polarization state). In this case, the difference between group velocities can typically be ignored. The two polarization components are now coherently coupled and the relative optical phase, phase velocity differential, and coherent energy exchange between the orthogonal polarization components must be retained. Theoretical analysis has found three lowest order stationary solutions for the low birefringence case; two fundamental soliton solutions that are linearly polarized along either the fast or slow axes [Eqs. (2a) and (2b)] and a (numerical) elliptically polarized solution.[13–15] The elliptically polarized solution is a PLVS because it contains energy in both components and propagates without change to its polarization state. The components have a relative phase of $\pm\pi/2$ but do not necessarily have amplitude profiles of the same functional shape. Hence, the polarization state is not uniform across the pulse.[13–15] Other higher order stationary solutions have also been found.[10,11,14] The elliptically polarized solitons possess a weak oscillatory instability, in contrast to solitons that are linearly polarized along the fast axis, which are unstable.[18]

For a PLVS to survive propagation with constant polarization state, the phase velocities of the two components must be identical. As shown in Fig. 1(b), a nonlinear index difference is created by an unequal distribution of energy between the two axes. The resulting difference (or nonlinear birefringence) in the nonlinear index compensates the linear birefringence exactly. This means that the phase velocities of the two axes are identical.

The magnitude of the nonlinear birefringence depends on the difference between the intensities of the components, i.e., the ellipticity of the polarization state since the relative phases must be $\pm\pi/2$. Thus, the ellipticity of the polarization state depends directly on the linear birefringence γ. Within the approximation of equal component profiles, this can be expressed as

$$|V|^2-|U|^2=\frac{\gamma}{g}, \tag{3}$$

where U and V are the time integrated amplitudes of u and v, $g\approx\frac{4}{3}q(1-A)$, and q is a soliton parameter that is inversely proportional to the soliton period and proportional to the square of the pulse energy.[12,13] Equation (3) also shows that $|V|^2\geqslant|U|^2$ with the component along the fast axis possessing greater intensity. The magnitude of the nonlinear birefringence of a pulse is limited by its energy and width (implicitly here through normalization) such that a PLVS cannot exist for linear birefringence $\gamma>(|V|^2+|U|^2)g$. Equivalently, this limit occurs as $|U|^2\to 0$ and the polarization state approaches linear polarization along the fast axis.

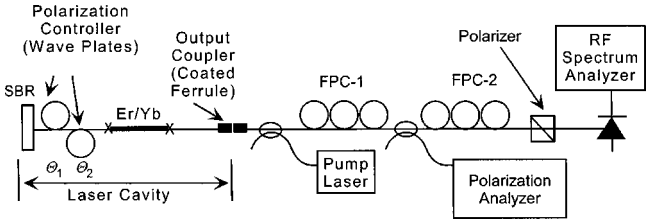

FIG. 2. Schematic diagram of the experiment (FPC, fiber polarization controller, SBR, saturable Bragg reflector, RF, radio frequency).

For large values of linear birefringence, a soliton that is linearly polarized along the fast axis [Eq. (2b)] becomes unstable. Instability of the fast axis due to nonlinearity was first described for CW propagation.[17] It also occurs for solitons,[18] and has been carefully addressed using soliton perturbation theory.[13] Because the fast axis is unstable, a pulse that is initially polarized along it will evolve away from it towards the slow axis, which is a stable point, and typically undergo oscillations around it. Because our fiber laser is nonconservative, the oscillations are damped, resulting in a solitons that are linearly polarized along the slow axis. The role played by nonlinearity provides an important distinction between the fast axis instability and the PLVS. In absence of nonlinearity, the PLVS states are not stable and do not exist, i.e., nonlinearity creates a new state. In contrast, nonlinearity destroys the stability of the fast axis, resulting in only a single stable state (the slow axis).

III. EXPERIMENT

Figure 2 shows the experiment. It consists of two parts, the fiber laser and the measurement apparatus.

A. Fiber laser

The fiber laser is described in more detail in Ref. 30. These measurements have been performed on several implementations of the laser with essentially identical results; the details vary from laser to laser (mainly the fiber lengths). Any specific numbers apply to the laser on which the bulk of the measurements present here were made. The laser cavity consists of two lengths of standard single mode fiber and a 17 cm piece of Er/Yb codoped fiber. The latter provides optical gain. The net round-trip cavity length is approximately 430 cm, corresponding to a repetition rate of 48 MHz. Modelocking is started and stabilized by a semiconductor passive saturable absorber known as a saturable Bragg reflector (SBR).[31] The SBR is butt-coupled to one end of the linear cavity and acts as a saturable high reflecting mirror. Solitonlike pulse shaping occurs in the cavity and dominates the steady state characteristics of the pulse. This is evidenced by the clean sech^2 optical spectrum (see Fig. 3). The average group velocity dispersion (GVD) of the cavity is +14.5 ps/nm/km (anomalous dispersion). Stable pulses are produced with a pulse width that can be adjusted by changing the pulse energy. As the pulse energy is varied from 160 to 65 pJ (by adjusting the pump power), the pulse width varies from 350 to 800 fs (FWHM) as expected for a fundamental

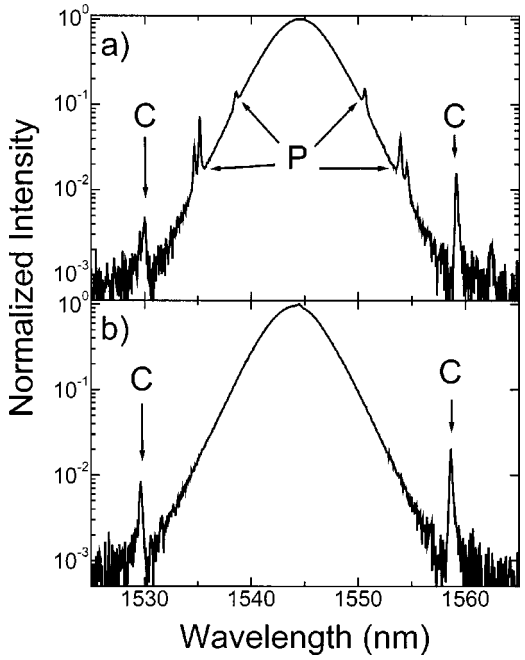

FIG. 3. Optical spectrum of the output pulse for (a) nonpolarization locked and (b) polarization locked operation. The side bands marked as ''C'' are due to the periodic perturbation by the cavity, while those marked as ''P'' are due the periodic perturbation of the polarization.

soliton. We estimate the total loss (and hence saturated gain) per round trip to be $<3\%$. The saturated reflectivity of the SBR is approximately 99.5% with $<0.5\%$ modulation due to saturation of the absorption. If the SBR is replaced with an ordinary dielectric high reflector, the laser operates CW.

The end of the cavity opposite from the SBR consists of a dielectric mirror that is coated directly onto the end of the fiber. This mirror is designed to be $\sim 99\%$ reflective at 1550 nm and high transmission at 980 nm. It serves as an output coupler, and allows light from a 980 nm laser diode to be coupled into the cavity to optically pump the Er atoms in the gain fiber. A wavelength-division multiplexer combines the 980 nm pump light into the fiber containing the output.

The soliton period, assuming a linearly polarized pulse, is given by[25]

$$z_0 = \frac{\pi \tau_0^2}{2|\beta_2|}, \tag{4}$$

where τ_0 is the pulse width and β_2 is the GVD. For the shortest pulses (350 fs), $z_0 = 3.5$ m, i.e., approximately the round-trip length of the cavity. For the longest pulses, $z_0 = 20$ m. Periodic perturbations to a soliton cause side bands in the optical spectrum.[32,33] The side bands marked by ''C'' in Fig. 3 are due to the periodic perturbation by the cavity (we will discuss the other sidebands later). Their relatively small magnitude ($<0.1\%$ of total energy) shows that the soliton is not strongly perturbed as it circulates in the cavity.

The linear birefringence in the cavity is controlled by wrapping a portion of the cavity fiber around two 5.5 cm diameter disks (these are known as fiber polarization controller paddles).[34] Each disk has three wraps, which for standard single mode fiber, provides approximately $\pi/2$ total linear retardation at 1550 nm with the fast axis in the bend plane of the fiber, i.e., they act like quarter waveplates. We specify the azimuthal angles, θ_1 and θ_2, of these paddles relative to a common arbitrary reference plane (i.e., the table). The remainder of the fiber constituting the laser cavity is mechanically secured so that the magnitude and principal axes of its birefringence (due to bends, strain, splices, etc.) is constant. We can determine the magnitude of the residual birefringence (see below) and find it to be less than $\pi/4$, typically around $\pi/8$. The total cavity birefringence is dominated by the paddles and by adjusting θ_1 and θ_2, we can adjust the retardance from 0 to slightly greater than 2π. Approximately 60% of the cavity fiber is contained in the paddles and these lengths are considerably shorter than the soliton period. Therefore, we are justified in characterizing the total cavity retardance by its net value.

B. Measurement apparatus

The measurement apparatus allows us to determine if the pulses are evolving, and how rapidly, as they circulate in the cavity, the azimuthal orientation of the principal axes in the cavity and the complete output polarization state for conditions where the polarization does not evolve. The measurement of the rate of polarization evolution is equivalent to measuring the cavity retardance.

As the pulse circulates in the cavity, its polarization state evolves under the influence of the net (linear plus nonlinear) birefringence in the cavity. The polarization state is effectively sampled each time the pulse reflects off of the output coupler and a small amount is emitted. To measure the evolution of the polarization, we pass the output through a linear polarizer and measure the transmitted intensity with a fast, polarization insensitive photodiode. The linear polarizer maps the evolution of the polarization into amplitude modulation (shown schematically in Fig. 4). We detect the amplitude modulation by measuring the radio-frequency (RF) spectrum of the signal emitted by the photodiode and observing the frequencies of the resulting side bands.

To show analytically that the linear polarizer maps the polarization evolution into amplitude modulation, consider the vector electric field of the pulse, $\mathbf{E}(z,t)$. For simplicity, we will assume that the polarization of the pulse evolves as a unit; i.e., the temporal profile is identical along the two principal axes. We then write

$$\mathbf{E}(z,t) = (E_x(z)\hat{\mathbf{x}} + E_y(z)\hat{\mathbf{y}})a(t'), \tag{5}$$

where $\hat{\mathbf{x}}$ and $\hat{\mathbf{y}}$ are unit vectors along the principal axes, $E_x(z)$ and $E_y(z)$ are complex amplitudes along the two direction, and $a(t')$ is an envelope function with $t' = t - (n/c)z$, where n is the average index of refraction and c is the speed of light. After propagation over a distance Δz, the electric field is

$$\mathbf{E}(z+\Delta z,t) = [E_x(z)e^{i\gamma\Delta z}\hat{\mathbf{x}} + E_y(z)e^{-i\gamma\Delta z}\hat{\mathbf{y}}]a(t')e^{i(n/c)\Delta z}. \tag{6}$$

The pulse is sampled every time it impinges on the output coupler, i.e., at $z = ml_c = m(c/n)\tau$, where m is an integer, l_c

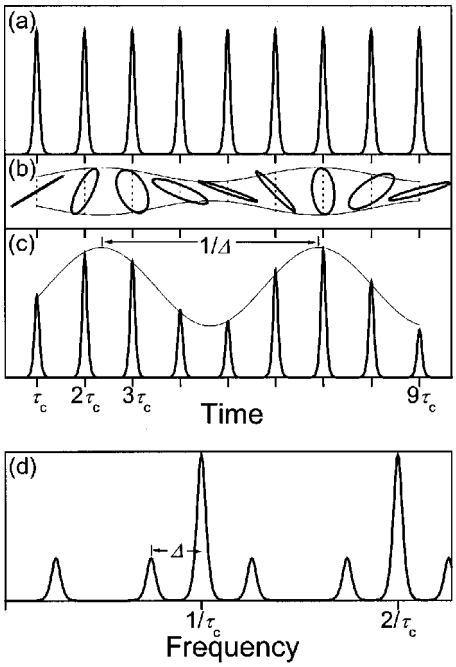

FIG. 4. Schematic of the conversion of polarization evolution into amplitude modulation by a linear polarizer. (a) The pulse train without polarization analysis. (b) The projection of each ellipse along the polarizer axis is shown by dashed lines. The resulting amplitude as a function of time is also shown. (c) The pulse train after polarization analysis showing the amplitude modulation. (d) The spectrum of the pulses in (c) showing the sidebands due to the amplitude modulation.

is the round trip length of the cavity, τ is the period; we have chosen the output coupler as the spatial origin. A linear polarizer with azimuthal angle θ relative to the $\hat{\mathbf{x}}$ axis projects these fields, resulting in a scalar electric field,

$$E(t)=(\cos(\theta)E_x(0)e^{i\gamma m(c/n)\tau} + \sin(\theta)E_y(0)e^{-i\gamma m(c/n)\tau})a(t-m\tau)e^{im\tau}. \quad (7)$$

The photodiode detects intensity $I(t)$,

$$I(t)=|E(t)|^2 = \left\{[\cos\theta E_x(0)]^2+[\sin\theta E_y(0)]^2 + 2E_x(0)E_y(0)\cos\theta\sin\theta\cos 2\gamma\frac{c}{n}t\right\}\delta(t-m\tau), \quad (8)$$

where we have assumed that the pulse is sufficiently short so that it can be approximated as a delta function. This is a train of delta functions in time with an amplitude modulation imposed on them at a frequency of $\Delta=\gamma c/n\pi$. This is shown schematically in Fig. 4. The spectrum of Eq. (8) will consist of a series of spikes, spaced by the cavity repetition frequency. Each spike has side bands at frequencies Δ. The product $\Delta\tau_c$ is the number of round trips required for the pulse to undergo a full evolution or total of 2π retardance. Hence the magnitude of the total round-trip cavity birefringence is $\beta=2\pi\Delta\tau_c=2l_c\gamma$ (in radians). From this we can see that measuring Δ is equivalent to measuring either β or γ. For a cavity birefringence of larger than π, Δ is aliased to below $1/(2\tau_c)$ because the polarization is only sampled once per round trip. Typical RF spectra with and without the polarizer are shown in Fig. 5. The side bands are clear.

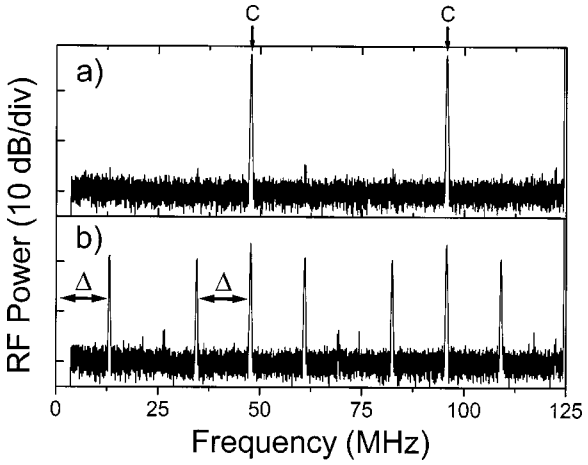

FIG. 5. RF spectra (a) without and (b) with the linear polarizer. The side bands are clearly evident in (b) and Δ is marked.

From Eq. (8) it can readily be seen that, if the polarizer is aligned along either principal axis ($\theta=0$, $\pi/2$), the amplitude modulation is not present. Hence, we can determine the orientation of the cavity axes by rotating the polarizer until the sidebands vanish. However, this measurement does not determine which axis is fast and which is slow.

In circumstances where the polarization is not evolving, it is useful to have a complete characterization of the polarization state. This is obtained by using a commercial polarization state analyzer.

To be useful, both the measurement of the cavity axes and the complete polarization state need to be made on the light at the output coupler. Any birefringence in the fiber intervening between the output coupler and the measurement apparatus will change the polarization state. It is therefore necessary to use fiber polarization controllers to compensate the birefringence. These controllers are similar to that used inside the cavity, but have three paddles configured to be approximately quarter-wave, half-wave, and quarter-wave retarders. These are set by disconnecting the laser, launching a series of known polarizations into the fiber and adjusting the fiber polarization controllers until the polarization states are reproduced at the measuring device.[23]

IV. CAVITY BIREFRINGENCE MEASUREMENT AND POLARIZATION LOCKING

The most basic measurement is to determine the polarization evolution frequency, Δ, as we adjust the angles θ_1 and θ_2 of the polarization controller paddles inside the laser cavity. The results are shown in Fig. 5.

As mentioned above, the measurement of Δ is equivalent to measuring the round trip retardance of the laser cavity. The overall structure of $\Delta(\theta_1,\theta_2)$ is well reproduced if total cavity birefringence is calculated using a Jones vector formulation.[20] The retardance of the paddles and the residual birefringence (retardance and axis orientation) used in the

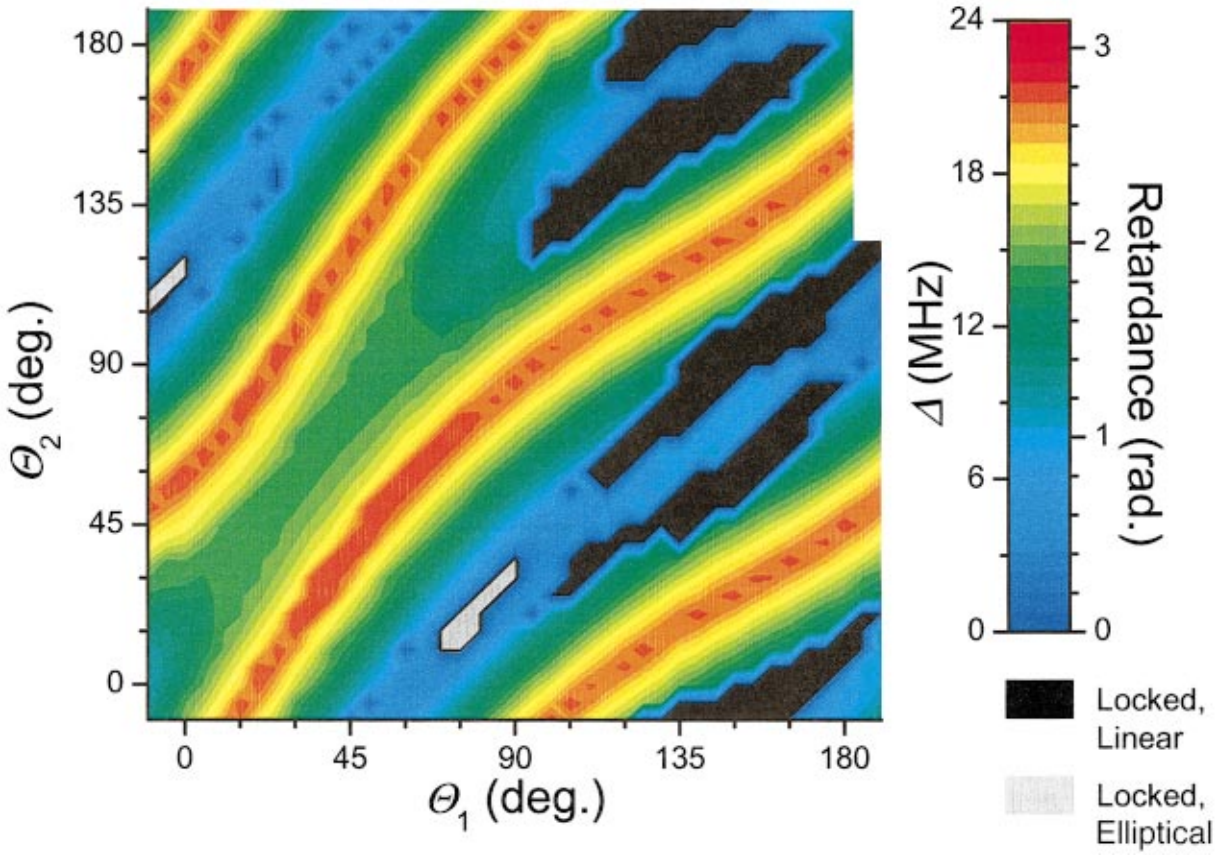

FIG. 6. (Color) The polarization evolution frequency, Δ, as function of the azimuthal angles of the two paddles θ_1 and θ_2. The correspondence between Δ and the net intracavity retardance is shown in the legend.

calculation are adjusted to obtain agreement with the data. The paddle retardance is found to be slightly under the design value of a quarter wave. The data shown in Fig. 6 are taken with the laser modelocked, the overall structure of $\Delta(\theta_1, \theta_2)$ is identical if the SBR is replaced with a high-reflector so that the laser runs CW. This demonstrates that nonlinear birefringence is weak.

For certain values of intracavity birefringence, the polarization evolution ceases, i.e., the side bands evident in Fig. 5 disappear. This indicates that the polarization is locked and not evolving as the pulse circulates in the cavity. These regions are shown in Fig. 6. The cavity still has net nonzero retardance, which is confirmed by making measurements of Δ when the laser is operating CW.

In Fig. 7, the region where the polarization locking occurs is enlarged and sampled with finer resolution in θ_1 and θ_2. In addition, the measurements are made at two different pulse energies. The pulse energy dependent size and positions of the regions, suggests that nonlinearity is responsible for the polarization locking. This is confirmed by the fact that locking is not observed when the laser is operating CW.

As described above, there are two mechanisms that can lead to pulses with a fixed state of polarization: polarization-locked vector solitons and the fast axis instability. These are differentiated by their polarization; PLVS have elliptical polarization, while the axis instability results in linear polarization. Upon measuring the polarization state in the locked regions, we discover that the region centered about zero retardance is elliptically polarized, while those centered at finite values of retardance are linearly polarized. Based on these observations, we tentatively assign the elliptically polarized regions to the formation of PLVS and the linearly polarized regions to the fast axis instability. We confirm these assignments in the following sections.

The two optical spectra shown in Fig. 3 are for cases where the polarization is (a) unlocked and (b) locked. Comparison of these spectra is interesting because of the appearance of additional side bands in the unlocked case (denoted by ''P'' in the figure). These sidebands are caused by the periodic perturbation of the polarization. Their positions depend on the intracavity birefringence in an analogous fashion to Δ. The optical sidebands are due to phase matching of the radiation shed by the soliton as it adjusts to perturbations.[32,33] It is believed that radiation shed due to random perturbation of the polarization will represent an ultimate limit in very high-speed soliton communication systems.[35] The presence of these polarization-induced sidebands is direct evidence that the polarization perturbations do cause solitons to radiate.

V. POLARIZATION LOCKED VECTOR SOLITONS

To verify that the locked regions with elliptical polarization are due to the formation of PLVS, we first make further detailed measurements of their properties. With these mea-

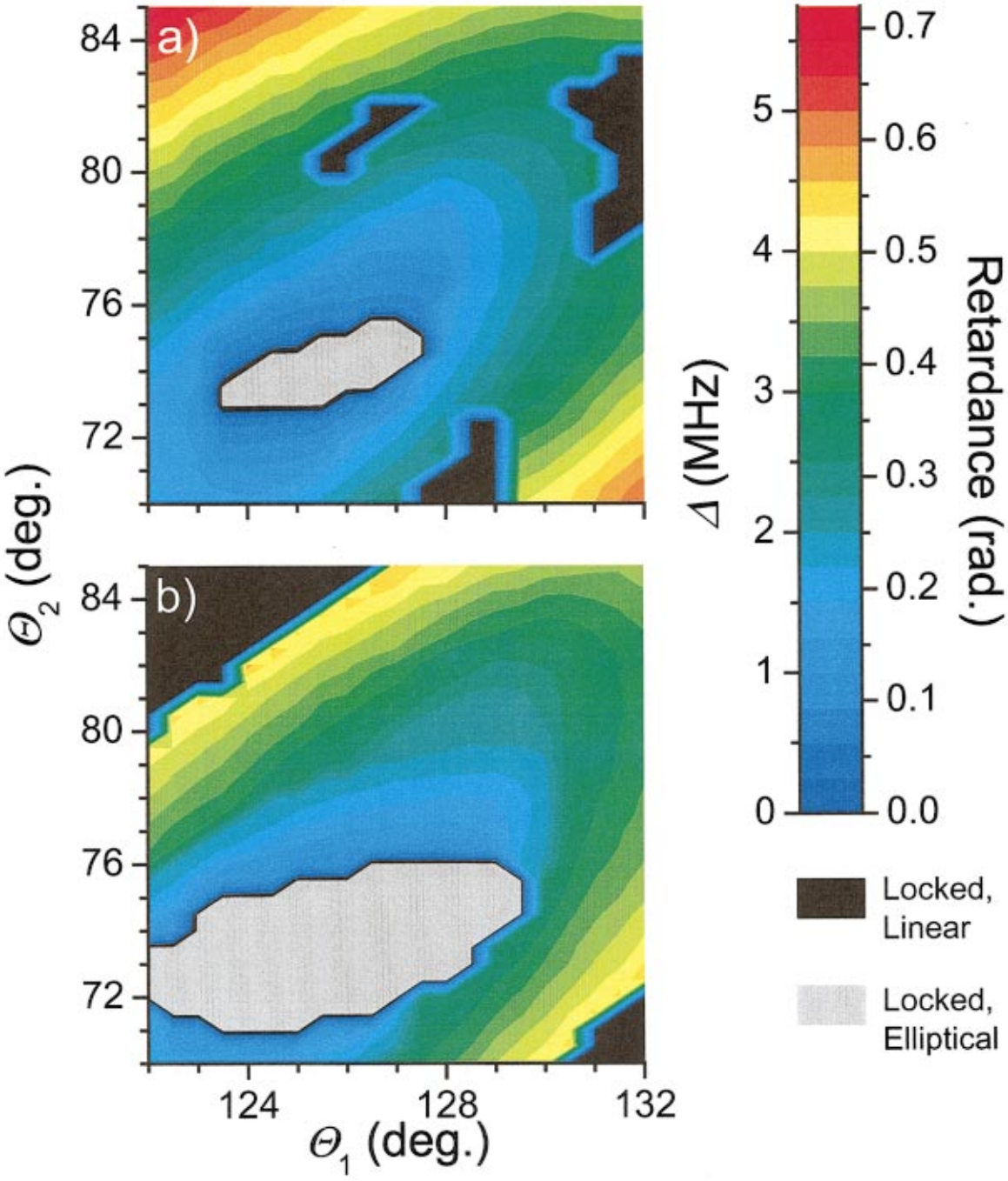

FIG. 7. (Color) Enlargement of region near zero retardance at (a) low and (b) high pulse energy.

surements, we can then understand why the exact compensation of linear birefringence by nonlinear birefringence is stable. This understanding provides confirmation that these regions are indeed due to PLVS formation.

A. Detailed characterization

It is most natural to characterize the output polarization state as a function of the intracavity birefringence (retardance and principal axes orientation). To provide a map from the angle of polarization controller paddle(s) to birefringence, we first operate the laser CW and measure the birefringence. Although the laser is no longer modelocked, we can still measure Δ with a sensitive radio frequency spectrum analyzer and environmental perturbations (i.e., tapping on the table), which causes modebeating and hence the time-varying output necessary for the polarization evolution to be evident. To simplify the measurement, we hold θ_1 fixed and only vary θ_2. However, we do choose θ_1 such that we can make the net retardance essentially zero by only varying θ_2. We estimate the total retardance to verify that we are working close to zero retardance not 2π, which aliases to 0 due to the finite sampling.

With the laser modelocked, we measure the complete polarization state (all Stokes parameters) of the output as a function of θ_2 using the polarization analyzer. The handed-

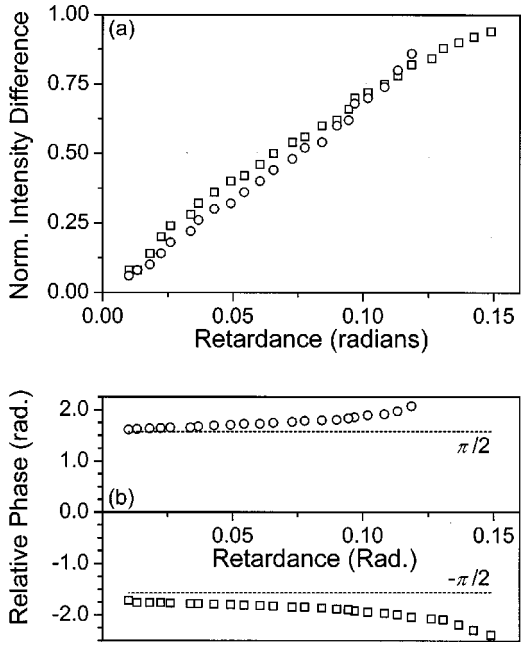

FIG. 8. The (a) intensity difference and (b) relative phase of the components of the PLVS as a function of retardance. Both handednesses are shown (circles and squares).

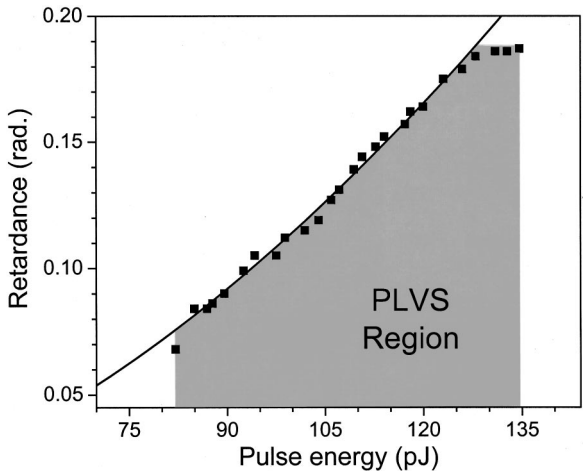

FIG. 9. Maximum round trip retardance for which elliptical locking is observed as function of the pulse energy. The solid line is proportional to the square of the pulse energy.

ness of the elliptically locked output depends on the direction (in θ_1, θ_2 space) from which the locked region was entered. The amplitude and relative phase of the components along the principal axes are determined by projecting the total measured polarization state onto the previously determined principal axes. The difference between the intensities of the components and their relative phase are plotted in Figs. 8(a) and 8(b). θ_2 has been converted to retardance and the results for both handedness outputs are plotted. As expected from Eq. (3) for a PLVS, the intensity difference shown in Fig. 8(a) depends linearly on the retardance. Furthermore, the measured relative phase is approximately constant at $+\pi/2$ or $-\pi/2$, as expected for a PLVS.

The relative phase deviates from the expected values of $\pm\pi/2$ for large values of cavity retardance. We believe that this deviation is due to the location of the output coupler relative to the location of the majority of the retardance, which is at the opposite end of the cavity. Since the balance is struck between the average linear and nonlinear birefringence, and the nonlinear birefringence is effectively distributed through out the cavity, local deviation away from a phase of $\pm\pi/2$ will occur. Moreover, this deviation is expected to be greater with increasing total linear birefringence as occurs in Fig. 5(b).

As evident in Fig. 6, the size of region, over which the elliptical locking occurs, depends on the pulse energy. The intracavity pulse energy is controlled by the pump power. Figure 9 plots the maximum value of birefringence where locking is observed as a function of pulse energy. At this point, the normalized intensity difference is typically within 5% of unity. This dependence agrees with Eq. (3) because higher levels of birefringence cannot be compensated once the normalized intensity difference reaches unity. Thus, the maximum birefringence that may be compensated, and for which a PLVS can exist, is dependent on the square of the pulse energy. Experimentally, the location of the edge of the elliptical locking region displays this form of dependence as indicated by the solid line in Fig. 9.

Figure 4 shows that the intensity of the optical spectrum has a hyperbolic secant form. Careful fitting to the spectrum as a function of frequency shows that this is true over four orders of magnitude.[23] Numerical PLVS solutions to the CNLSE possess a polarization state that varies temporally across the pulse.[12,14,24] Physically, this occurs because of a difference in power between the two principal axes. For zero retardance, the polarization state is circular and the two profiles are identical. For increasing birefringence, the component along the fast axis increases in intensity and therefore must become shorter in time (wider in spectrum). This behavior is observed experimentally. We oriented the linear polarizer along each principal axis (as described above) and replaced the photodiode with an optical spectrum analyzer. In Fig. 10, the spectral bandwidth along both axes is plotted as a function of intracavity birefringence. As expected, near zero birefringence, the two components are of comparable

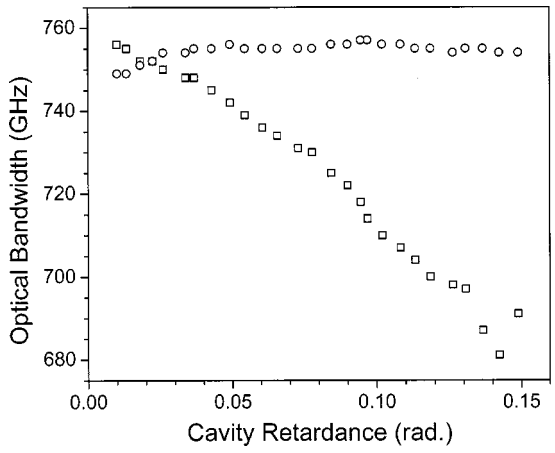

FIG. 10. Optical bandwidth as a function of retardance for fast (circles) and slow (squares) principal axes.

widths. With increasing cavity retardance, the component along the fast axis maintains a wider spectral width, which is in agreement with simulations (see below).

B. Stability mechanism

The extensive measurements are all in agreement with the expectations for PLVS; we therefore conclude that they are forming in the regions where the locked polarization is elliptical. As described above, the PLVS depends on a delicate balance between linear and nonlinear birefringence. Their stability requires the suppression of both amplitude and phase perturbations. A change of one of the component's amplitude translates into a constant drift of their relative phase through the unbalanced linear and nonlinear birefringences, resulting in polarization evolution. Likewise, a perturbation in relative phase causes energy transfer between components via the coherent energy coupling. This in turn results in an amplitude perturbation. Therefore, since the PLVS are stable in the cavity, a mechanism stabilizing the PLVS against perturbations must exist.

The combined action of coherent energy coupling, SPM, and XPM provides the negative feedback necessary for stability. The direction and magnitude of the energy transferred between components by the coherent energy coupling depends on the relative phase of the components. For a relative phase of $\pm\pi/2$ there is no energy transfer. Thus, if the energy is already distributed properly for the nonlinear birefringence to compensate the linear birefringence, a relative phase of $\pm\pi/2$ represents a stationary point, in agreement with the experimentally observed relative phase. Perturbations away from this point are corrected because energy is transferred from the component lagging in phase to the component leading in phase. This increases the nonlinear phase shift (the nonlinear index of refraction) of the leading component and brings it back into phase with the lagging component.

Amplitude perturbations are corrected in a similar fashion. If the amplitude of one component is slightly too large, it begins to lag in phase due to the larger nonlinear shift. This results in a transfer of energy from it to the other component, returning their amplitudes back to the correct relative value.

This mechanism provides negative feedback that provides a restoring force towards a relative phase of $\pm\pi/2$ and the correct amplitude distribution such that the nonlinear birefringence exactly compensates the linear birefringence. However, it only provides a restoring force and does not provide any damping. Therefore any perturbation will result in oscillations about the stable point. Any disturbance will oscillate between the phase and amplitude. Numerical solutions of the strictly conservative CNLSE exhibit such oscillatory behavior.[14] However, the experimentally observed PLVS are stationary and stable, therefore perturbations must be damped. We conjecture that the nonconservative elements in the laser (gain and loss, both of which are weakly nonlinear) are responsible for suppressing the oscillatory behavior. Numerical simulations that incorporate nonconservative terms also exhibit stable nonoscillatory behavior.[21,24]

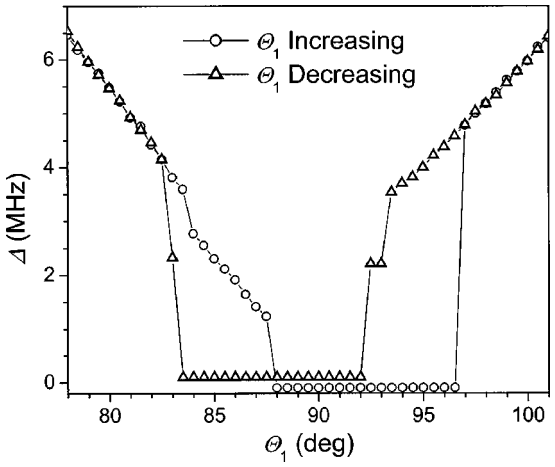

FIG. 11. Polarization evolution frequency, Δ, as function of θ_1 for θ_1 increasing (circles) and θ_1 decreasing (triangles). Elliptical polarization locking (PLVS) is represented by $\Delta=0$, the data are offset vertically in the PLVS region for clarity.

In general, any form of phase locking often results in hysteretic behavior. For the PLVS, if the difference in the phase velocities is too high, the locking cannot occur because the power does not redistribute quickly enough to achieve a locked state. However once a locked state is achieved, the difference between the linear phase velocities can be slowly increased and the locking mechanism will compensate. We observe just such hysteresis. In Fig. 11, the polarization evolution frequency is plotted as function of θ_1. At the edges of the locking region, hysteresis occurs. In these regions the laser is actually tristable, the possible states are unlocked (polarization evolving) and locked with relative phases of $\pm\pi/2$ (i.e., left- and right-hand elliptical polarization).

C. Simulations

Numerical simulations of this fiber laser are presented in detail in Ref. 24. In this section, we briefly reproduce some of the results to show that the simulations agree with the experimental results.

The laser is theoretically modeled with two coupled complex Ginzburg–Landau equations that include fiber birefringence, spectral filtering, saturable gain, and slow saturable loss. The basic model includes a gain/loss anisotropy that is absent in the experiment. This is because the nonconservative terms for each component depend only on the respective component. The model can be made isotropic numerically. This is done by evaluating the gain/loss terms along all possible azimuthal directions.

Figure 12 shows the theoretically predicted energy difference between the two components [equivalent experimental data is in Fig. 8(a)]. Figure 13 shows the theoretically predicted stability boundary for the PLVS (equivalent experimental data are in Fig. 9). Figure 14 shows the theoretically predicted spectral widths (equivalent experimental data are in Fig. 10).

These results demonstrate the good agreement between the theoretical and experimental results.

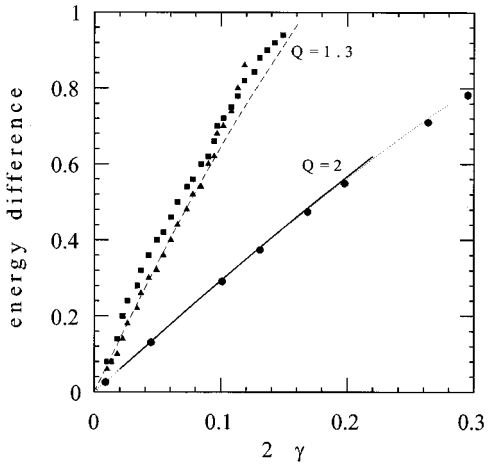

FIG. 12. Theoretically predicted pulse energy difference between the components polarized along the principal axes. Q denotes pulse energy which is determined by the nonconservative term in the theory. The $Q=2$ result is compared to the conservative result (circles). The $Q=1.3$ result agrees very well with the experiment [squares and triangles correspond to the data in Fig. 8(a)]. (Reproduced from Ref. 24 with the permission of the authors.)

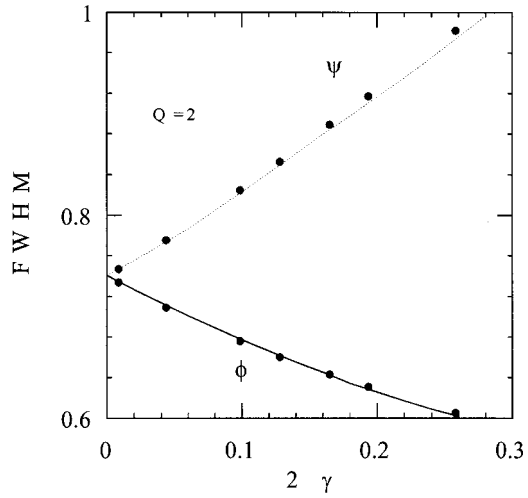

FIG. 14. Theoretically predicted spectral widths of the two components as a function of phase velocity difference. (Reproduced from Ref. 24 with the permission of the authors.)

VI. FAST AXIS INSTABILITY

In the purely linear regime, the principal axes of a birefringent material represent stable points for linearly polarized light. This means that if light that is linearly polarized, or nearly so, is launched along one of the two axes, it will maintain both its degree of polarization and orientation with respect to the axis. This is the basis for polarization maintaining fiber, which has a large amount of birefringence manufactured into it.

However, when the nonlinear index of refraction is considered the picture becomes more complex. If linearly polarized light is aligned with the slow axis, the nonlinear increase of the index adds to the magnitude of the linear birefringence and enhances the stability of the slow axis. In contrast, if linearly polarized light is aligned with the fast axis, the nonlinear increase in the index of refraction can compensate the linear birefringence, possibly even switching the axes. This is shown schematically in Fig. 1(c). This second case is clearly unstable; the effective axis is determined by the polarization direction of the light, not by the axes of the linear birefringence. Hence there will be no restoring force to correct for perturbation. The instability of the fast axis has been analyzed for CW light[17] and solitons.[18] Evidence for it has been observed in soliton propagation experiments.[19] The instability will only occur if the retardance is in a certain range, which depends on pulse energy. If the linear retardance is too small, then the nonlinear birefringence overwhelms it and neither axis is stable. For very large values of retardance, the nonlinear index can be ignored and the system behaves as if only linear birefringence is present.

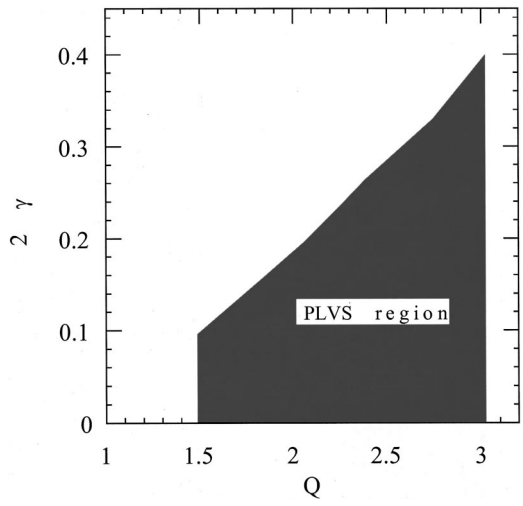

FIG. 13. Theoretically predicted stability boundary for the PLVS. (Reproduced from Ref. 24 with the permission of the authors.)

We observe the instability of the fast axis as polarization locked states that are linearly polarized along the slow axis. This occurs for certain values of birefringence, as shown in Figs. 6 and 7. The polarization analyzer allows us to readily determine that the output in these states is linearly polarized. As described above, we can also easily determine the position of the cavity axes and verify that the output is aligned with a cavity axis. However, the measurement apparatus does not allow us to directly identify the axes.

To determine the identity of the axes, we utilize the PLVS. Within the regions where the PLVS form, the identity of the axes is clear because the higher intensity component must be aligned with the fast axis. Thus, we can begin in the PLVS and vary θ_1 and θ_2 until we reach a region where the output is locked and linearly polarized. By carefully tracking the orientation of the fast and slow axes as θ_1 and θ_2 are adjusted, we can identify them for any value of θ_1 and θ_2. The assignment of the fast and slow axes is verified by estimating their positions from the positions and measured retardance of the paddles.

The angle of the slow axis and the angle of linearly polarized locked output is shown in Fig. 15(a) as a function of θ_2. This clearly shows that the polarization of the output is aligned along the slow axis in the linearly locked regions. The linearly polarized output can be nulled by a crossed

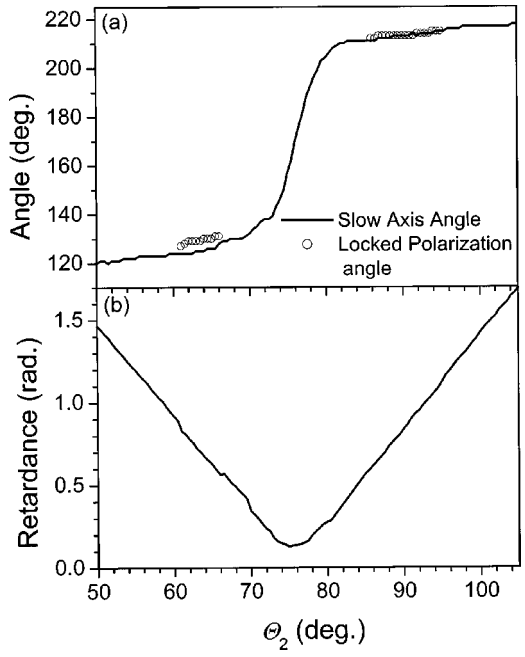

FIG. 15. (a) The measured azimuthal angle of the slow axis (line) and the azimuthal angle of the linearly polarized locked output (circles) as function of θ_2. (b) The corresponding measured retardance as function of θ_1.

polarizer by more than a factor of 5000, indicating that the polarization state varies by less than 0.04% across the pulse shape.

As expected, the range of retardance where the axis instability occurs depends on pulse energy. This is shown in Fig. 16. For larger pulse energy, the region is larger and the center shifts to larger values of birefringence. The converse occurs for decreasing pulse energy. The discussion above explains this behavior.

These results clearly demonstrate that the locked, linearly polarized output is due to the instability of the fast axis.

Linearly polarized locking also occurs when the net cavity retardance is greater than π but less than 2π. However, in these regions the polarization is aligned along the fast axis. We conjecture that, since nonlinear effects tend to only respond to the average birefringence, a fast axis with a retardance of $2\pi-\epsilon$ (where $\pi \ll \epsilon < 2\pi$) can appear to the nonlinear pulse as an effective slow axis with a retardance of ϵ. Thus the relative phase between the components can slip by 2π each roundtrip. To achieve $\sim 2\pi$ of average cavity birefringence, the polarization controller paddles must dominate the total cavity birefringence since each offers only a roundtrip retardation of π. Therefore, the large birefringence is lumped into approximately half the cavity with the 2π phase slip occurring over a short distance compared to the length scale of the nonlinearity.

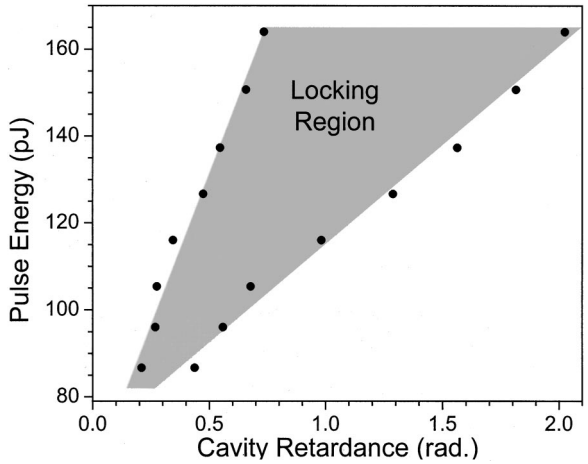

FIG. 16. Plot of the upper and lower values of retardance for which linear locking occurs as function of cavity retardance.

VII. SUMMARY

We have observed that the output of a modelocked fiber laser can lock its polarization state for certain settings of the intracavity birefringence. We have performed extensive experiments to determine the underlying physical mechanism. For very low values of birefringence, the output is elliptically polarized and we assign the locking to the formation of polarization locked vector solitons. For slightly larger retardance, the output is linearly polarized and we assign the locking to the instability of the fast axis.

We have obtained a relatively complete understanding of what is occurring in the fiber laser. Theoretical simulations provide good agreement with the experiment. Because the round trip gain and loss in the fiber laser is small, it provides a better approximation to a conservative system than that provided by a standard telecommunications long distance transmission system. It also provides essentially infinite propagation distance. We believe that both of these are necessary to enable our observations.

ACKNOWLEDGMENTS

The authors would like to thank all of the colleagues with whom we have discussed this work over the last few years. We specifically acknowledge the contributions of Nail Akhmediev and Jose Soto-Crespo. Their theoretical work contributed immensely towards achieving a solid understanding of the physical mechanisms underlying polarization locked vector solitons. We also acknowledge the support of Wayne Knox throughout this project.

[1] A. Hasegawa and F. Tappert, ''Transmission of stationary nonlinear optical pulses in dispersive dielectric fibers. I. Anomalous dispersion,'' Appl. Phys. Lett. **23**, 142 (1973).
[2] I. P. Kaminow, ''Polarization in optical fiber,'' IEEE J. Quantum Electron. **I7**, 15 (1981).
[3] L. F. Mollenauer, R. H. Stolen, and J. P Gordon, ''Experimental observation of picosecond narrowing and solitons in optical fiber,'' Phys. Rev. Lett. **45**, 1095 (1980).
[4] H. A. Haus and W. S. Wong, ''Solitions in optical communications,'' Rev. Mod. Phys. **68**, 423 (1996).
[5] C. D. Poole and J. Nagel, ''Polarization effects in lightwave systems,'' in *Optical Fiber Telecommunications IIIA*, edited by I. P. Kaminow and T. L. Koch (Academic, San Diego, 1997), p. 114.
[6] M. N. Islam, C. D. Poole, and J. P. Gordon, ''Soliton trapping in birefringent optical fibers,'' Opt. Lett. **14**, 1011 (1989).
[7] C. R Menyuk, ''Nonlinear pulse-propagation in birefringent optical fiber,'' IEEE J. Quantum Electron. **23**, 174 (1987).
[8] C. R Menyuk, ''Stability of soliton in birefringent optical fibers 1. Equal propagation amplitudes,'' Opt. Lett. **12**, 614 (1988).

[9] C. R Menyuk, ''Stability of soliton in birefringent optical fibers. 2. Arbitrary amplitudes,'' J. Opt. Soc. Am. B **5**, 392 (1989).
[10] D. N. Christodoulides and R. I. Joseph, ''Vector solitons in birefringent nonlinear dispersive media,'' Opt. Lett. **13**, 53 (1988).
[11] M. V Tratnik and J. E. Sipe, ''Bound solitary waves in a birefringent optical fiber,'' Phys. Rev. A **38**, 2011 (1988).
[12] N. Akhmediev, A. Buryak, and J. M. Soto-Crespo, ''Elliptically polarized solitons in birefringent optical fibers,'' Opt. Commun. **112**, 278 (1994).
[13] N. Akhmediev and J. M. Soto-Crespo, ''Dynamics of solitonlike pulses propagation in birefringent optical fibers,'' Phys. Rev. E **49**, 5742 (1994).
[14] N. N. Akhmediev, A. V. Buryak, J. M. Soto-Crespo, and D. R. Andersen, ''Phase-locked stationary soliton states in birefringent nonlinear optical fibers,'' J. Opt. Soc. Am. B **12**, 434 (1995).
[15] J. M. Soto-Crespo, N. Akhmediev, and A. Ankiewicz, ''Stationary solitonlike pulses in birefringent optical fiber,'' Phys. Rev. E **51**, 3547 (1995).
[16] Y. Chen and J. Atai, ''Femtosecond soliton pulses in birefringent optical fibers,'' J. Opt. Soc. Am. B **14**, 2365 (1997).
[17] H. G. Winful, ''Polarization instabilities in birefringent nonlinear media: Application to fiber-optic devices,'' Opt. Lett. **11**, 33 (1986).
[18] K. J. Blow, N. J. Doran, and D. Wood, ''Polarization instabilities for solitons in birefringent fibers,'' Opt. Lett. **12**, 202 (1987).
[19] Y. Barad and Y. Silberberg, ''Polarization evolution and polarization instability of solitions in a birefringent optical fiber,'' Phys. Rev. Lett. **78**, 3290 (1997).
[20] S. T. Cundiff, B. C. Collings, and W. H. Knox, ''Polarization locking in an isotropic, modelocked soliton Er/Yb fiber laser,'' Opt. Express **1**, 12 (1997).
[21] N. N. Akhmediev, J. M Soto-Crespo, S. T. Cundiff, B. C. Collings, and W. H. Knox, ''Phase locking and periodic evolution of solitons in passively mode-locked fiber lasers with a semiconductor saturable absorber,'' Opt. Lett. **23**, 852 (1998).
[22] S. T. Cundiff, B. C. Collings, N. N. Akhmediev, J. M. Soto-Crespo, K. Bergman, and W. H. Knox, ''Observation of polarization-locked vector solitons in an optical fiber,'' Phys. Rev. Lett. **82**, 3988 (1999).
[23] B. C. Collings, S. T. Cundiff, N. N. Akhmediev, J. M. Soto-Crespo, K. Bergman, and W. H. Knox, ''Polarization-locked temporal vector solitons in a fiber laser: Experiment,'' J. Opt. Soc. Am. B **17**, 354 (2000).
[24] J. M. Soto-Crespo, N. N. Akhmediev, B. C. Collings, S. T. Cundiff, K. Bergman, and W. H. Knox, ''Polarization-locked temporal vector solitons in a fiber laser: Theory,'' J. Opt. Soc. Am. B **17**, 366 (2000).
[25] G. V. Agrawal, *Nonlinear Fiber Optics* (Academic, San Diego, 1995), pp. 263–265.
[26] S. V. Manakov, ''On the theory of two-dimensional self-focusing of electromagnetic waves,'' Sov. Phys. JETP **38**, 248 (1974).
[27] J. U. Kang, G. I. Stegeman, J. S. Atchison, and N. Akhmediev, ''Observation of Manakov spatial solitons in AlGaAs planar waveguides,'' Phys. Rev. Lett. **76**, 3699 (1996).
[28] S. G. Evangelides, Jr., L. F. Mollenauer, J. P. Gordon, and N. S. Bergano, ''Polarization multiplexing with solitons,'' J. Lightwave Technol. **10**, 28 (1992).
[29] L. F. Mollenauer, K. Smith, J. P. Gordon, and C. R. Menyuk, ''Resistance of solitons to the effects of polarization dispersion in optical fibers,'' Opt. Lett. **14**, 1219 (1989).
[30] B. C. Collings, K. Bergman, S. T. Cundiff, S. Tsuda, J. N. Kutz, M. Koch, and W. H. Knox, ''Short cavity erbium/ytterbium fiber lasers mode-locked with a saturable Bragg reflector,'' IEEE J. Sel. Top. Quantum Electron. **3**, 1065 (1997).
[31] S. Tsuda, W. H. Knox, S. T. Cundiff, W. Y. Jan, and J. E. Cunningham, ''Mode-locking ultrafast solid-state lasers with saturable Bragg reflectors,'' IEEE J. Sel. Top. Quantum Electron. **2**, 454 (1996).
[32] S. M. J. Kelley, ''Characteristic side-band instability of periodically amplified average soliton,'' Electron. Lett. **28**, 806 (1992).
[33] J. P. Gordon, ''Dispersive perturbation of solitons of the nonlinear Schrödinger equation,'' J. Opt. Soc. Am. B **9**, 91 (1992).
[34] H. C. Lefevre, ''Single-mode fiber fractional wave devices and polarization controllers,'' Electron. Lett. **16**, 778 (1980).
[35] A. Hasegawa (personal communication).